10.1515/acsc-2017-0003

Archives of Control Sciences
Volume 27(LXIII), 2017
No. 1*, pages 41–62*

Robust H_∞ output feedback control of bidirectional inductive power transfer systems

AKSHYA SWAIN, DHAFER ALMAKHLES, MICHAEL J. NEATH and ALIREZA NASIRI

Bidirectional Inductive power transfer (IPT) systems behave as high order resonant networks and hence are highly sensitive to changes in system parameters. Traditional PID controllers often fail to maintain satisfactory power regulation in the presence of parametric uncertainties. To overcome these problems, this paper proposes a robust controller which is designed using linear matrix inequality (LMI) techniques. The output sensitivity to parametric uncertainty is explored and a linear fractional transformation of the nominal model and its uncertainty is discussed to generate a standard configuration for μ-synthesis and LMI analysis. An H_∞ controller is designed based on the structured singular value and LMI feasibility analysis with regard to uncertainties in the primary tuning capacitance, the primary and pickup inductors and the mutual inductance. Robust stability and robust performance of the system is studied through μ-synthesis and LMI feasibility analysis. Simulations and experiments are conducted to verify the power regulation performance of the proposed controller.

Key words: inductive power transfer, wireless power transfer, robust control, Linear Matrix Inequalities, sensitivity analysis

1. Introduction

Wireless power transfer technology (WPT) is an efficient method of delivering power between two physically isolated systems either through means of a time-varying magnetic field (e.g. Inductive Power Transfer (IPT)) or through the use of electric field coupling (e.g. Capacitive Power Transfer (CPT)). These technologies allow power transfer to take place in environments unsuited for conventional means of energy transfer, and various circuit topologies have been successfully proposed and implemented to cater for a wide range of applications from low power designs for bio-medical implants to high power battery charging systems [27, 5, 17, 14, 16]. Their resilience to harsh external conditions have led to an increase of IPT systems found in areas such as materials handling, renewable energy and heating in recent times [18, 3]. IPT systems for electric

A. Swain (e-mail: a.swain@auckland.ac.nz), the corresponding author, and M.J. Neath (neathmj@gmail.com) are with Department of Electrical and Computer Engineering, The University of Auckland, New Zealand. D. Almakhles (dalmakhles@gmail.com) is with Prince Sultan University, Riyadh, Saudi Arabia. A. Nasiri (nassirym@yahoo.com) is with Hormozgan University, Bandar Abbas, Iran.

Received 4.12.2016.

vehicles (EVs) have been a focal point of interest in recent years, to meet the growing demand for renewable energy. Bidirectional IPT systems are ideal for vehicle-to-grid (V2G) and G2V applications as they are more tamper proof and are able to function in harsh weather conditions [37, 24].

Bidirectional IPT systems suffer significant performance degradation when detuned and thus parallel and series compensations are typically used to improve the power-handling capabilities of IPT systems, causing the systems to behave as high-order resonant networks [29, 26, 11]. As a consequence, IPT systems are complex in nature and are difficult to both design and control when maintained at an operating frequency of 10-100 kHz [36]. Two separate controllers are required to facilitate power flow across the coils, which are dedicated to controlling the converters of either side of the system. In contrast to unidirectional systems, bidirectional IPT systems are even higher order resonant networks and more complex.

In the past, most IPT systems have utilised various types of controllers including directional tuning, fuzzy, bit-stream and simple PI and PID controllers as a means of verifying a model or particular control strategy [7, 6, 9, 10, 8, 12, 13, 31, 32]. These controllers give sub-optimal performance if not correctly tuned and are vulnerable to system disturbances and parametric variations which are prevalent in such systems. Recently the authors in [23] have applied multi-objective genetic algorithms to tune the PID parameters. Such controllers are also associated with tedious tuning processes often involving trial and error, motivating a model based robust controller design approach to overcome such problems.

In recent years, H_∞ controllers have gained popularity as a solution to the low robustness of PID controllers [35, 21]. Robust controllers for uni-directional systems have been developed in [19], where the authors have designed a robust controller for frequency uncertainty. Further, the Linear Matrix Inequality (LMI) framework has been used to design optimal robust controllers which both satisfies robustness as well as the necessary performance parameters [25, 39, 15]. This paper proposes a model based design approach of an H_∞ robust controller for bi-directional IPT systems which can effectively reduce the effects of uncertainties of the system parameters. Due to the complexity of optimal H_∞ controllers, the proposed controller, designed using the LMI method, is reduced to a 2nd order polynomial during the experimental stage. The rest of the paper is organised as follows: Section 2 describes the bidirectional IPT system in detail including the dynamic model of the system . The controller design and synthesis as well as the modelling of uncertainties are described in section 3. Simulation and experimental results are presented in Section 4 with conclusions in Section 5.

2. Bidirectional IPT system

A typical bidirectional IPT system consists of a primary and a secondary side and is shown in Fig. 1. Both sides contain identical circuitry including a converter, an inductor-capacitor-inductor (LCL) resonant network with a series capacitor and dedicated con-

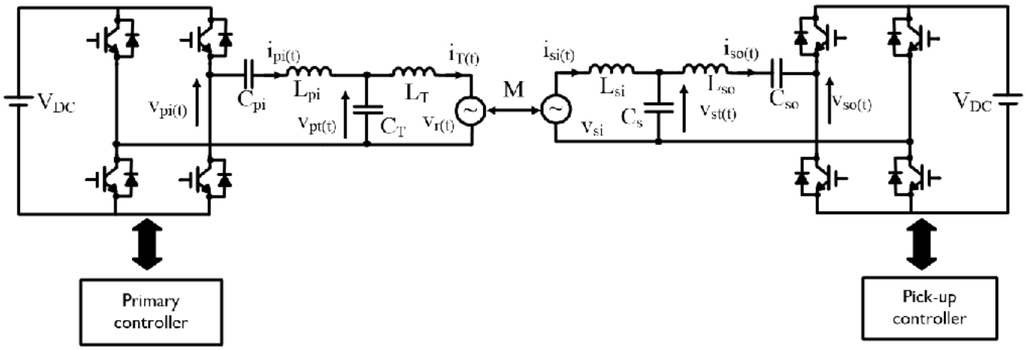

Figure 1: Typical bidirectional IPT system

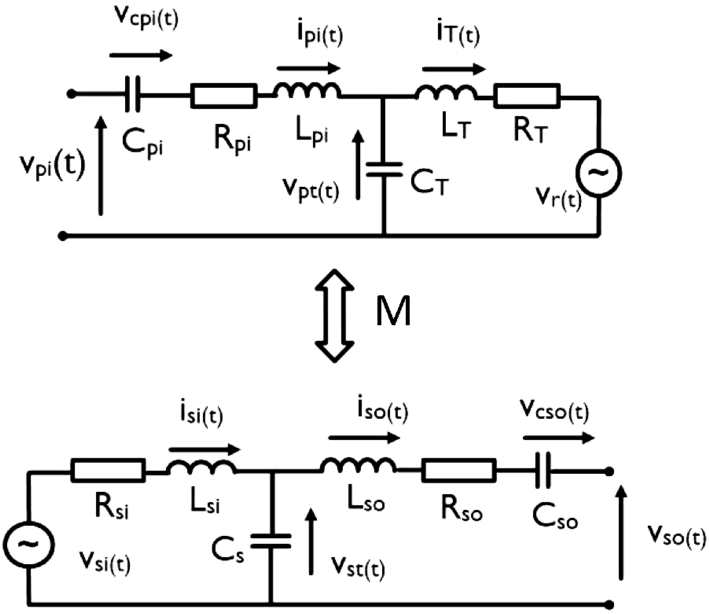

Figure 2: Equivalent circuit of a bidirectional system

troller which operates independently. The primary side converter generate a sinusoidal current at a desired frequency f_0 in the primary winding L_{pt}. Both LCL circuits are tuned to the frequency of the primary track current i_{pt}. A voltage is induced in the secondary pickup coil L_{st} as it is magnetically coupled with the primary. The voltage vectors are controlled by varying the phase angle α which in turn controls the voltage of the system. A phase angle difference of ± 90 degrees results in maximum power transfer, where a leading phase angle constitutes power transfer from the secondary to the primary and likewise a lagging phase angle enables power transfer from the primary to the secondary.

2.1. Dynamic model

Fig. 2 shows the bidirectional IPT system represented in schematic form. The dynamic model of this circuit developed in [34, 30, 33] is described as :

$$x = \begin{bmatrix} x_1 & x_2 & x_3 & x_4 & x_5 & x_6 & x_7 & x_8 \end{bmatrix}^T = \begin{bmatrix} i_{pi} & v_{cpi} & v_{pt} & i_T & i_{so} & v_{cso} & v_{st} & i_{si} \end{bmatrix}^T$$

where:

i_{pi} – current through the primary side inductor L_{pi}
v_{cpi} – voltage across the primary input capacitor C_{pi}
v_{pt} – voltage across primary side capacitor C_T
i_T – current through track inductor L_T
i_{so} – current through the pick-up side inductor L_{so}
v_{cso} – voltage across the pick-up output capacitor C_{so}
v_{st} – voltage across the pick-up side capacitor C_s
i_{si} – current through the pick-up side inductor L_{si}

Let the input vector u be denoted as:

$$u = \begin{bmatrix} u_1 & u_2 \end{bmatrix}^T = \begin{bmatrix} v_{pi} & v_{so} \end{bmatrix}^T$$

where $u_1 = v_{pi}$ is the input voltage applied at the primary side. Note that this voltage is essentially the output voltage of the primary side converter and $u_2 = v_{so}$= voltage at the pick-up side. Following the basic principles of circuit theory, the dynamic model can be expressed by the 8 differential equations as follows:

$$\begin{aligned}
\dot{x}_1 &= -\frac{R_{pi}}{L_{pi}}x_1 - \frac{1}{L_{pi}}x_2 - \frac{1}{L_{pi}}x_3 + \frac{1}{L_{pi}}u_1 \\
\dot{x}_2 &= \frac{1}{C_{pi}}x_1 \\
\dot{x}_3 &= \frac{1}{C_T}x_1 - \frac{1}{C_T}x_4 \\
\dot{x}_4 &= \gamma\left[\frac{1}{L_T}x_3 - \frac{R_T}{L_T}x_4 - \beta x_7 - \beta R_{si}x_8\right] \\
\dot{x}_5 &= -\frac{R_{so}}{L_{so}}x_5 - \frac{1}{L_{so}}x_6 + \frac{1}{L_{so}}x_7 - \frac{1}{L_{so}}u_2 \\
\dot{x}_6 &= \frac{1}{C_{so}}x_5 \\
\dot{x}_7 &= -\frac{1}{C_s}x_5 + \frac{1}{C_s}x_8 \\
\dot{x}_8 &= \gamma\left[\beta x_3 - \beta R_T x_4 - \frac{1}{L_{si}}x_7 - \frac{R_{si}}{L_{si}}x_8\right]
\end{aligned} \tag{1}$$

where

$$\beta = \frac{M}{L_{si}L_T}, \quad \gamma = \frac{1}{1-M\beta}$$

This can be expressed in the standard state space form as :

$$\dot{x} = Ax + Bu \tag{2}$$

where the system matrix A is given by

$$A = \begin{bmatrix} \frac{-R_{pi}}{L_{pi}} & -\frac{1}{L_{pi}} & -\frac{1}{L_{pi}} & 0 & 0 & 0 & 0 & 0 \\ \frac{1}{C_{pi}} & 0 & 0 & 0 & 0 & 0 & 0 & 0 \\ \frac{1}{C_T} & 0 & 0 & -\frac{1}{C_T} & 0 & 0 & 0 & 0 \\ 0 & 0 & \frac{\gamma}{L_T} & -\frac{\gamma R_T}{L_T} & 0 & 0 & -\gamma\beta & -\gamma\beta R_{si} \\ 0 & 0 & 0 & 0 & -\frac{R_{so}}{L_{so}} & -\frac{1}{L_{so}} & \frac{1}{L_{so}} & 0 \\ 0 & 0 & 0 & 0 & \frac{1}{C_{so}} & 0 & 0 & 0 \\ 0 & 0 & 0 & 0 & -\frac{1}{C_s} & 0 & 0 & \frac{1}{C_s} \\ 0 & 0 & \gamma\beta & -\gamma\beta R_T & 0 & 0 & -\frac{\gamma}{L_{si}} & -\frac{\gamma R_{si}}{L_{si}} \end{bmatrix}$$

and the input matrix B is given by

$$B = \begin{bmatrix} \frac{1}{L_{pi}} & 0 & 0 & 0 & 0 & 0 & 0 & 0 \\ 0 & 0 & 0 & 0 & -\frac{1}{L_{so}} & 0 & 0 & 0 \end{bmatrix}^T \tag{3}$$

Considering the track current $i_T = x_4$ and pick-up current $i_{so} = x_5$ as outputs, the output equation can be written as:

$$y = Cx \tag{4}$$

where

$$y = \begin{bmatrix} y_1 & y_2 \end{bmatrix}^T = \begin{bmatrix} i_T & i_{so} \end{bmatrix}^T, \quad C = \begin{bmatrix} 0 & 0 & 0 & 1 & 0 & 0 & 0 & 0 \\ 0 & 0 & 0 & 0 & 1 & 0 & 0 & 0 \end{bmatrix} \tag{5}$$

The relative gain array (RGA) analysis performed in [30] suggests strong interaction between output y_1 and input u_1 as well as between output y_2 and input u_2. From this it can be seen that the system can be controlled using a decentralized approach. It should also be noted that this is the ideal control configuration as it will allow the primary and secondary sides to be controlled independently without the need for communication.

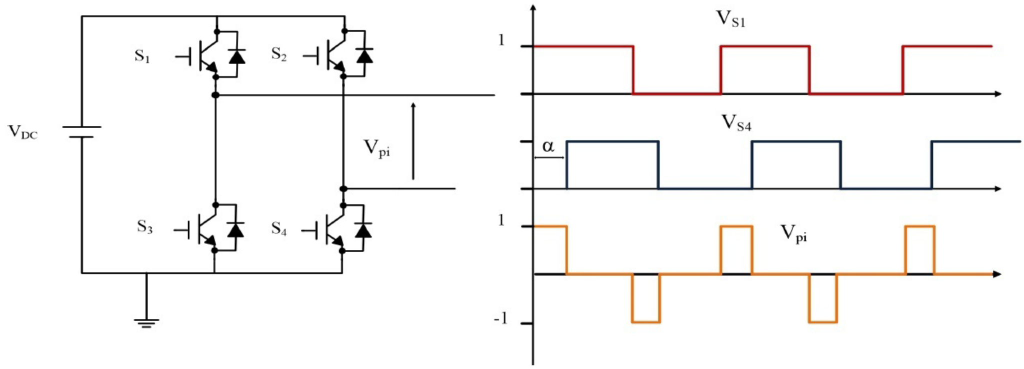

Figure 3: Waveforms for H-Bridge switching

3. Bidirectional IPT pickup-side controller

Robustness is a crucially important component of control theory, as real engineering systems are vulnerable to external disturbances, measurement noise and modeling uncertainties. In terms of IPT systems, uncertainties and disturbances may cause frequency drifts, loss of efficiency or instability. One typical source of uncertainty is the discrepancy between the mathematical model and the physical system.

As inferred from the relative gain array analysis, decentralized control is an acceptable method for obtaining the desired response. Therefore, the proposed controller ensures the control of the secondary side only, whilst the primary side controller is operated at a fixed phase angle using an open-loop controller. The pickup controller regulates the output power P_{si} by varying the voltage v_{si} applied to the secondary side's resonant network as [23]:

$$P_{si} = \frac{M}{L_{st}} \frac{\|v_{pi}\|}{\omega Lpt} \|v_{si}\| \sin(\theta) \tag{6}$$

Voltage v_{si} can be controlled by varying the secondary side phase angel α_s. The voltage produced by the pick up converter can be expressed in terms of α_s as :

$$v_{si} = V_{sin} \frac{4}{\sqrt{2}\pi} \sin(\alpha_s) \tag{7}$$

where V_{sin} is the dc voltage of the active load supplied by the pickup-side converter. Fig. 3 shows how the interaction between the angle α and the input switching signals. It can be seen from this that variations in αchange the output voltage V_{pi} by varying its duty cycle.

3.1. Singular value sensitivity

The concept of sensitivity is very useful in the analysis and controller design for feedback systems [22, 1, 2]. An important issue in designing a controller for an IPT system is the sensitivity of outputs to parameter variations. It is therefore appropriate to conduct a sensitivity analysis of the system to quantify the effect of variations of system parameters on the overall system model and provide better insight on controller behaviour when exposed to disturbances.

Singular value sensitivity is an effective method for quantifying the effect the parametric uncertainties on the system model. Suppose the transfer function matrix (TFM) of the nominal system is $G_0(j\omega)$. Let the TFM of the real system be $G'(j\omega)$. Then,

$$\Delta G(j\omega) = G^{'}(j\omega) - G_0(j\omega) \tag{8}$$

$G_0(j\omega)$ differs from $G^{'}(j\omega)$, by a variation in parameter p by an amount Δp. The sensitivity of a particular value σ from its nominal value σ_0 due to variations of a paramenter p is defined as:

$$S_p^{\sigma}(j\omega) = \frac{\Delta\sigma}{\sigma_0} \cdot \frac{p}{\Delta p} \tag{9}$$

For a perturbed system, the limits of the output are bounded by $\bar{\sigma}(G^{'}(j\omega))$ and $\underline{\sigma}(G^{'}(j\omega))$. Similarly the maximum and minimum deviations of the output are bounded by $\bar{\sigma}(\Delta G(j\omega))$ and $\underline{\sigma}(\Delta G(j\omega))$. Table 1 shows the singular value sensitivities for a range of variations in system parameters, where the percentage change in maximum value $\Delta\sigma(\%)$ is defined by

$$\Delta\sigma(\%) = \frac{\bar{\sigma}(G^{'}(j\omega)) - \bar{\sigma}(G_0(j\omega))}{\bar{\sigma}(G_0(j\omega))} \times 100 \tag{10}$$

The magnitude of the sensitivity of the maximum singular values is defined as:

$$\left\| S_p^{\sigma}(j\omega) \right\| (\%) = \left\| \frac{\bar{\sigma}(G\text{'}(j\omega)) - \bar{\sigma}(G_0(j\omega))}{\bar{\sigma}(G_0(j\omega))} \right\| \cdot e \left\| \frac{p}{\Delta p} \right\| \tag{11}$$

Table- 1 shows parameters computed by varying the primary tuning capacitance C_T, primary track inductance L_T and secondary inductance L_{si} at 20kHz. It can be concluded that bidirectional IPT systems are very sensitive to changes in the tuning capacitance, which can be attributed to the fact that C_T is used as the tuning capacitance for both inductors of the LCL circuit. The sensitivity of the system to variations in the pickup inductance is lower for the same reason as well as due to changes in the magnetic coupling. This further validates the need for a robust controller that adequately deals with parametric uncertainties.

3.2. Modelling of uncertain systems

In many robust design problems, the uncertainties include unstructred uncertainties such as unmodelled dynamics and parameter variations. Many dynamic perturbations that occur in different parts of a system can be lumped into one single perturbation block Δ. Through the use of linear fractional transformations (LFTs), the uncertain parts can

Table 1: Sensitivity of singular value for variations in L_T , L_{si} and C_T for bidirectional IPT system

	% change in parameter	$\triangle\bar{\sigma}(\%)$	$S_p^{\bar{\sigma}}(\%)$
L_T	−20	5.99	14.98
	−10	2.92	14.6
	10	−2.47	13.85
	20	−5.37	13.42
L_{si}	−20	2.69	6.725
	−10	0.95	4.75
	10	−0.54	2.7
	20	−0.76	1.94
C_T	−20	−12.7	63.37
	−10	−6.83	68.29
	10	8.022	80.22
	20	17.6	87.83

be taken out of the dynamics and the whole system can be arranged in the standard linear fractional transformation $F_u(M,\Delta)$ [4].

In a realistic system, the three physical parameters C_T,L_T and L_{si} are not exactly known. However, it can be assumed that these values are within certain known intervals, represented as:

$$\begin{aligned} C_T &= C_{T_0}(1+p_c\delta_c) \\ L_T &= C_{T_0}(1+p_t\delta_t) \\ L_{si} &= L_{si_0}(1+p_s\delta_s) \end{aligned} \tag{12}$$

where C_{T_0}, L_{T_0}, and L_{si_0} are the nominal values for C_T,L_T and L_{si} respectively. p_c,p_t,p_s and δ_c,δ_t,δ_s represent the relative perturbations on these parameters. In the present study, it is assumed that $C_{T_0} = 2.49\mu F$, $L_{T_0} = 22.84\mu H$,$L_{si_0} = 23.49\mu H$, $p_c = 0.2$,$p_t = 0.4$ and $p_s = 0.4$ and $-1 \leqslant \delta_c\delta_t\delta_s \leqslant 1$. This represents ±40% uncertainty in the primary and pickup inductors L_T and L_{si} and ±20% uncertainty in the primary tuning capacitance C_T. Variations in L_T and L_{si} also vary the mutual inductance M according to

$$M = k\sqrt{L_T L_{si}} \tag{13}$$

and can be modelled by an LFT formulation in terms of β, as can variations in parameters $\frac{1}{C_T}$, $\frac{1}{L_T}$ and $\frac{1}{L_{si}}$ in terms of p , δ and their nominal values. Many dynamic perturbations that occur in different parts of a system can be lumped into one single perturbation block Δ. Through the use of linear fractional transformations (LFTs), the uncertain parts can be taken out of the dynamics and the whole system can be arranged in the standard linear fractional transformation [4, 28] as shown in Fig 4, where the block Δ denotes the model uncertainty and G_{mod} denotes the nominal model which is dependent on the existing state space model as well as on C_{T_0}, L_{T_0}, L_{si_0} and β_0 .

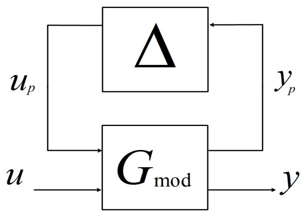

Figure 4: Uncertain model of the Bi-directional IPT system

The dynamic behavior of the nominal system can be described as:

$$\begin{aligned} \dot{x} &= Ax(t) + B_1 u_p(t) + B_2 u(t) \\ y_p(t) &= C_1 x(t) + D_{11}(t) + D_{12} u(t) \\ y(t) &= C_2 x(t) + D_{12} u_p(t) + D_{22} u(t) \end{aligned} \tag{14}$$

where $x \in \mathbf{R}^n$ is the state variable vector, $u \in \mathbf{R}^m$ is the system input, $y \in \mathbf{R}^r$ is the measurement output and $u_p \in \mathbf{C}^p$ and $y_p \in \mathbf{C}^p$ are uncertainty signals described by

$$\begin{aligned} u_p &= \begin{bmatrix} u_{c1} & u_{c2} & u_{L1} & u_{L2} & u_{s1} & u_{s2} & u_{b1} & u_{b2} & u_{b3} & u_{b4} \end{bmatrix}^T \\ &= \begin{bmatrix} \delta_{c1} y_{c1} \\ \delta_{c2} y_{c2} \\ \delta_{L1} y_{L1} \\ \delta_{c2} y_{c2L2} \\ \delta_{s1} y_{s1} \\ \delta_{s2} y_{s2} \\ \delta_{b1} y_{b1} \\ \delta_{b2} y_{b2} \\ \delta_{b3} y_{b3} \\ \delta_{b4} y_{b4} \end{bmatrix} \end{aligned} \tag{15}$$

$$
\begin{aligned}
y_p &= \begin{bmatrix} y_{c1} & y_{c2} & y_{L1} & y_{L2} & y_{s1} & y_{s2} & y_{b1} & y_{b2} & y_{b3} & y_{b4} \end{bmatrix}^T \\
&= \begin{bmatrix} -p_c u_{c1} + \frac{1}{C_{T_0}} x_1 \\ -p_c u_{c2} + \frac{1}{C_{T_0}} x_4 \\ -p_L u_{L1} + \frac{\gamma}{L_{T_0}} x_3 \\ -p_L u_{L2} + R_T \frac{\gamma}{L_{T_0}} x_4 \\ -p_s u_{s1} + R_T \frac{\gamma}{L_{si_0}} x_7 \\ -p_s u_{s2} + R_{si} \frac{\gamma}{L_{si_0}} x_8 \\ \gamma\beta_0 x_7 \\ \gamma\beta_0 R_T x_4 \\ \gamma\beta_0 x_3 \\ \gamma\beta_0 R_{si} x_8 \end{bmatrix}
\end{aligned}
\tag{16}
$$

The matrices A,$B_2 = B$ and $C_2 = C$ are the system, input and output matrices respectively and B_1,C_1 and D are given by

$$
B_1 = \begin{bmatrix}
0 & 0 & 0 & 0 & 0 & 0 & 0 & 0 & 0 & 0 \\
0 & 0 & 0 & 0 & 0 & 0 & 0 & 0 & 0 & 0 \\
-p_c & p_c & 0 & 0 & 0 & 0 & 0 & 0 & 0 & 0 \\
0 & 0 & -p_l & p_l & 0 & 0 & -p_b & 0 & 0 & p_b \\
0 & 0 & 0 & 0 & 0 & 0 & 0 & 0 & 0 & 0 \\
0 & 0 & 0 & 0 & 0 & 0 & 0 & 0 & 0 & 0 \\
0 & 0 & 0 & 0 & 0 & 0 & 0 & 0 & 0 & 0 \\
0 & 0 & 0 & 0 & p_s & p_s & 0 & -p_b & -p_b & 0
\end{bmatrix}
\tag{17}
$$

$$
C1 = \begin{bmatrix}
\frac{1}{C_{T_0}} & 0 & 0 & 0 & 0 & 0 & 0 & 0 \\
0 & 0 & 0 & \frac{1}{C_{T_0}} & 0 & 0 & 0 & 0 \\
0 & 0 & \frac{\gamma}{L_{T_0}} & 0 & 0 & 0 & 0 & 0 \\
0 & 0 & 0 & \gamma\frac{R_T}{L_{T_0}} & 0 & 0 & 0 & 0 \\
0 & 0 & 0 & 0 & 0 & 0 & \frac{\gamma}{L_{si_0}} & 0 \\
0 & 0 & 0 & \gamma\beta_0 R_T & 0 & 0 & 0 & 0 \\
0 & 0 & \gamma\beta_0 & 0 & 0 & 0 & 0 & 0 \\
0 & 0 & 0 & 0 & 0 & 0 & 0 & \gamma\beta_0 R_{si}
\end{bmatrix}
\tag{18}
$$

$$
D_{11} = \begin{bmatrix}
-p_c & 0 & 0 & 0 & 0 & 0 \\
0 & -p_c & 0 & 0 & 0 & 0 \\
0 & 0 & -p_l & 0 & 0 & 0 \\
0 & 0 & 0 & -p_l & 0 & 0 \\
0 & 0 & 0 & 0 & -p_s & 0 \\
0 & 0 & 0 & 0 & 0 & -p_s
\end{bmatrix}
\tag{19}
$$

$$
D_{12} = D_{21}^T = 0_{(10\times 2)}, \qquad D_{22} = 0_{(2\times 2)}
\tag{20}
$$

The block diagram of the closed loop system is shown in Fig-5 where d is the disturbance on the system output with finite energy. W_1 is a weighting function which is selected to tailor the tracking requirement and similarly W_2 is used to ensure good noise rejection. The weighting functions are generally used because it is often undesirable

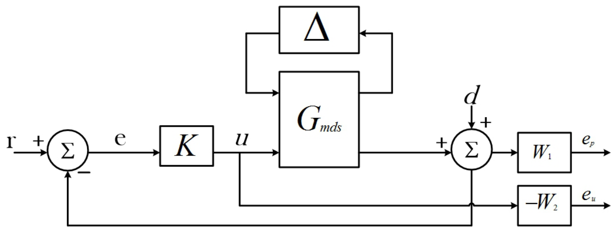

Figure 5: Block diagram of closed-loop system structure

and unfeasible to minimize the sensitivity over all frequencies. The weighting functions are chosen by the designer to tailor the tracking requirement and are usually high gain low pass filters. By applying the weights, instead of minimizing the sensitivity function alone, the weight W_1 is applied and $\| W_1 S \|_\infty$ is minimized. Similarly for good noise rejection, a control weighting function W_2 is used such that $\| W_2 KS \|_\infty$ is minimized [28, 4].

To obtain a good control design, it is necessary to select suitable weighting functions. The performance and control weighting functions that have been used in this work are given in the form [28]

$$W_1 = \frac{\beta(\alpha s^2 + 2\zeta\omega_c\sqrt{\alpha}s + \omega^2)}{(\beta s^2 + 2\zeta_2\omega_c\sqrt{\beta}s + \omega^2)} \tag{21}$$

$$W_2 = \frac{s^2 + 2\frac{w_{bc}}{\sqrt{M_u}} + \frac{\omega_{bc}^2}{M_u}}{\varepsilon s^2 + 2\sqrt{\varepsilon}\omega_{bc}s + \omega_{bc}^2} \tag{22}$$

where β is the d.c gain of the function which controls the disturbance rejection,α is the high frequency gain which controls the response peak overshoot, ζ_1 and ζ_2 are the damping ratios of the cross over frequency, ω_{bc} is the controller bandwidth, M_u is the peak magnitude of the sensitivity function and ε is a parameter chosen to be a small value which lies usually in the range 0.01 to 0.1.

3.3. Robust control design using Linear Matrix Inequalities

The formulation of the H_∞ synthesis problem can achieve a set of desired controllers by resolving a convex optimization problems with a set of linear matrix inequality (LMI) constraints in the form [38, 20].

$$F(x) \triangleq F_0 + \sum_{i=1}^{m} x_i F_i < 0 \tag{23}$$

Affine parameter dependent models are well suited for Lyapunov based analysis and synthesis, and can be used to analyse the stability and the performance of the uncertain systems. The objective of the output feedback controller is to satisfy the following properties:

1. It should be a stabilizing controller K, such that the system is always stable for any perturbations under the condition $\| \Delta \|_\infty \leqslant 1$

2. The H_∞ norm of the transfer function $T_{dz}(s)$ from the variable d to z should be less than 1, namely

$$\left\| \begin{array}{c} \mathrm{T}_{de_p}(s) \\ \mathrm{T}_{de_u}(s) \end{array} \right\|_\infty < 1 \tag{24}$$

The H_∞ performance can be optimized by solving the following LMI problem:

$$\begin{gathered}
\begin{bmatrix} N_{21} & 0 \\ 0 & I \end{bmatrix}^T \begin{bmatrix} A^T X + XA & XB_1 & C_1^T \\ B_1^T X & -\gamma I & D_{11}^T \\ C_1 & D_{11} & -\gamma I \end{bmatrix} \begin{bmatrix} N_{21} & 0 \\ 0 & I \end{bmatrix} < 0 \\
\begin{bmatrix} N_{12} & 0 \\ 0 & I \end{bmatrix}^T \begin{bmatrix} AY + XA^T & YC_1^T & B_1 \\ C_1 X & -\gamma I & D_{11} \\ B_1^T & D_{11}^T & -\gamma I \end{bmatrix} \begin{bmatrix} N_{12} & 0 \\ 0 & I \end{bmatrix} < 0 \\
\begin{bmatrix} X & I \\ I & Y \end{bmatrix}^T \geqslant 0
\end{gathered} \tag{25}$$

where N_{12} and N_{21} denote bases of null spaces of $\left(B_2^T, D_{12}^T\right)$ and (C_2, D_{21}) respectively. These terms are used to evaluate the parts that cannot be reflected by the measured output and cannot be affected by the control input. By solving the above LMI problem, the two positive definite matrices X and Y are found such that

$$X - Y^{-1} = X_2 X_2^T \tag{26}$$

Then, by applying the singular value decomposition to (26), we get the matrix $X_2 \in \mathbf{R}^{n \times n_k}$, where n_k can be the rank of $X - Y^{-1}$. Further a matrix X_c is constructed using X and X_2 as:

$$X_c = \begin{bmatrix} X & X_2^T \\ X_2 & I \end{bmatrix} \tag{27}$$

To solve a H_∞ synthesis controller, a matrix K composed by all unknown coefficient matrices is defined as:

$$K = \begin{bmatrix} A_k & B_k \\ C_k & D_k \end{bmatrix} \tag{28}$$

Lastly, a LMI, which is only dependant on the matrix K, will be be solved and this is given by

$$H_{X_C} + P_{X_C}^T KQ + Q^T K^T P_{X_C} < 0 \tag{29}$$

For inequality (29), the matrices H_{X_C},P_{X_C} and Q are all known and certain, having the forms of

$$H_{X_C} = \begin{bmatrix} A_0^T X_c + X_c A_0 & X_c B_0 & C_0^T \\ B_0^T X_c & -I & D_{11}^T \\ C_0 & D_{11} & -I \end{bmatrix} \tag{30}$$

$$P_{X_C} = \begin{bmatrix} \overline{B}^T X_c & 0 & \overline{D}^T \end{bmatrix} \tag{31}$$

$$Q = \begin{bmatrix} \overline{C} & D_{21} & 0 \end{bmatrix} \tag{32}$$

where A_o, B_o, C_o, $\overline{B}$, $\overline{C}$, $\overline{D}_{12}$ and $\overline{D}_{21}$ are respectively equal to

$$A_o = \begin{bmatrix} A & 0 \\ 0 & 0 \end{bmatrix}^T, \; B_o = \begin{bmatrix} B_1 \\ 0 \end{bmatrix}, \; C_o = \begin{bmatrix} C_1 & 0 \end{bmatrix}, \; \overline{B} = \begin{bmatrix} 0 & B_2 \\ I & 0 \end{bmatrix}$$

$$\overline{C} = \begin{bmatrix} 0 & I \\ C_2 & 0 \end{bmatrix}, \; \overline{D}_{12} = \begin{bmatrix} 0 & D_{12} \end{bmatrix}, \; \overline{D}_{21} = \begin{bmatrix} 0 \\ D_{21} \end{bmatrix}$$

The H_∞ synthesis problem can be transformed into a feasibility problem of a linear matrix inequality system only dependent on the control parameters to be solved. Thus it is easy to achieve an H infinity output feedback controller based on the LMI method.

4. Results

To demonstrate the effectiveness of the robust controller, a 1kW bidirectional IPT prototype shown in Fig. 9 was built as a benchmark. The various parameters of the prototype are shown in Table 2. Before performing the experiments, initial simulations were carried out where the step response of the system, controlled both with PID and H_∞ controllers, were compared. The simulations were then performed again with altered system parameters and finally conducted on the prototype. The phase shift θ is held constant at 90° and phase angle α is varied on the pick up side controller to regulate power flow between the primary and secondary coils.

4.1. Simulations

The response time of the H_∞ controller is investigated using PLECS, a MATLAB simulation-based software package. At time $t = 0$, a step change in reference voltage of ± 1.0kW is applied to the system corresponding to power flowing to and from the

Table 2: Parameters of Bidirectional IPT prototype converter

Parameter	Value
$V_{DC,1} = V_{DC,2}$	150V
$L_{pi} = L_{so}$	46.5μH
L_T	22.84μH
L_{si}	23.49μH
$C_T = C_s$	2.47μF
$C_{pi} = C_{so}$	2.53μF
M	5μH
f_0	20kHz

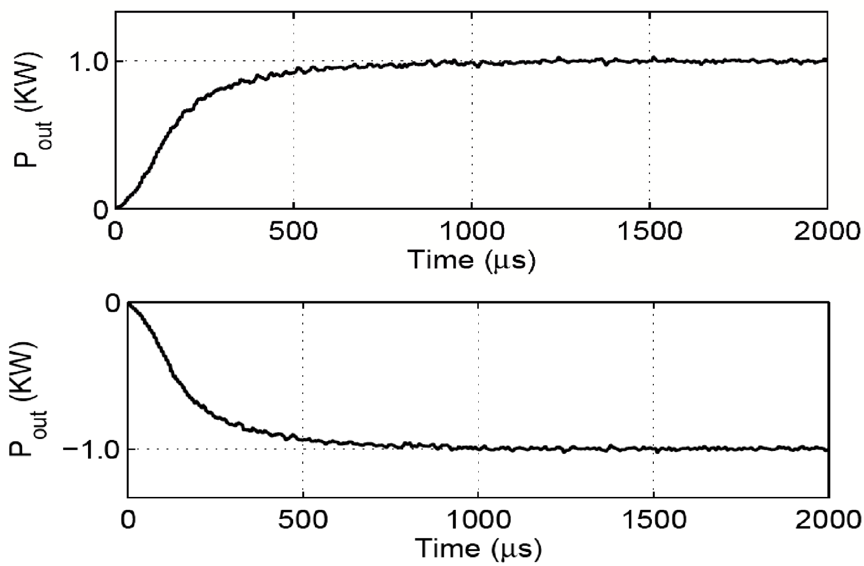

Figure 6: Power regulation performance of robust controller in forward and reversed direction

primary and secondary. Variations in C_T,L_T and L_{si} of 40% were introduced into the system. Fig. 6 shows the step response of the nominal system in forward and reverse direction.

The gain of the H_∞ controller designed using the methods described before can be represented as:

$$K(s) = \frac{U(s)}{E(s)} = \frac{\sum_{i=0}^{13} b_i s^i}{\sum_{j=0}^{13} a_i s^i} \tag{33}$$

where $a_0 = 0, a_1 = 5 \times 10^5, a_2 = 1.4 \times 10^5, a_3 = 1.1 \times 10^{49}, a_4 = 8.4 \times 10^{44}, a_5 = 3.0 \times 10^{40}$, $a_6 = 4.0 \times 10^{35}, a_7 = 1.2 \times 10^{31}, a_8 = 5.7 \times 10^8, a_9 = 1.7 \times 10^{21}, a_{10} = 2.6 \times 10^{10}, a_{11} = 7.4 \times 10^{11}, a_{12} = 3.6 \times 10^4$, $b_0 = 3.2 \times 10^{54}, b_1 = 9.2 \times 10^{51}, b_2 = 6.3 \times 10^{48}, b_3 = 1.2 \times 10^{45}, b_4 = 8.5 \times 10^{40}, b_5 = 2.4 \times 10^{36}$, $b_6 = 4.0 \times 10^{31}, b_7 = 9.32 \times 10^{26}, b_8 = 5.6 \times 10^{21}, b_9 = 1.2 \times 10^{17}, b_{10} = 2.5 \times 10^{10}, b_{11} = 5.4 \times 10^6, b_{12} = 3.6 \times 10^4, b_{13} = 7.2 \times 10^{-5}$.

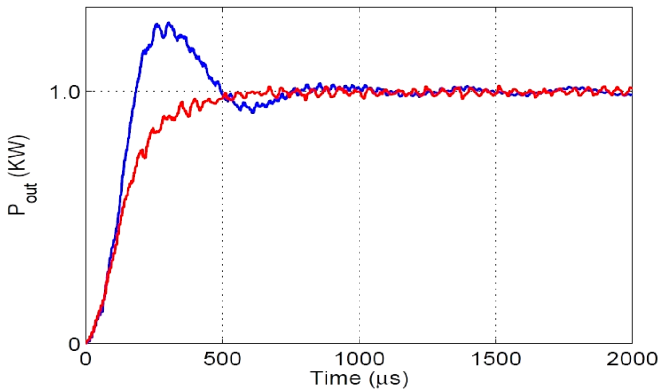

Figure 7: Comparison of power regulation for PID (blue) and robust (red) control systems with 40% variation in primary tuning capacitance C_T

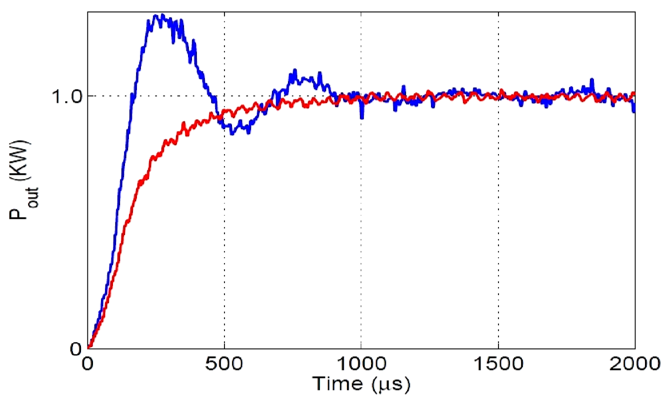

Figure 8: Comparison of power regulation for PID (blue) and robust (red) control systems with 40% variation in primary and pickup tuning inductances L_T and L_{si}

As shown in Figs 7 and 8, the PID controller shows significant decrease in performance in the presence of parametric disturbances. Both cases show increased overshoot and oscillations when a variation of 40% is introduced to the tuning capacitor and inductors, while the robust controller experiences no significant variations. Results for reverse direction are similar in nature and therefore not shown.

4.2. Experimental

To verify the results obtained from the MATLAB simulations, experiments were conducted on the prototype bidirectional IPT system, using a Texas Instruments TMS28335 microcontroller. The prototype is capable of transferring approximately 1kW of power over a 48mm air gap with 85% efficiency. The gain of the controller given in (33) in the discrete domain , when sampled at a rate of 40 kHz is given by

$$K(z) = \frac{U(z)}{E(z)} = \frac{\sum_{i=0}^{13} b_i z^i}{\sum_{j=0}^{13} a_i z^i} \tag{34}$$

where $a_0 = -0.4, a_1 = 1.7, a_2 = -3.2, a_3 = 5.3, a_4 = -8.0, a_5 = 9.6, a_6 = -10.8, a_7 = 11.7, a_8 = -10.2, a_9 = 8.9, a_{10} = -7.0, a_{11} = 4.0, a_{12} = -2.4, a_{13} = 1, b_0 = -1.9 \times 10^{-5}, b_1 = 9.2 \times 10^{-5}, b_2 = -1.9 \times 10^{-4}, b_3 = 3 \times 10^{-4}, b_4 = -4.8 \times 10^{-4}, b_5 = 5.8 \times 10^{-4}, b_6 = -6.5 \times 10^{-4}, b_7 = 7.3 \times 10^{-4}, b_8 = -6.4 \times 10^{-4}, b_9 = 5.5 \times 10^{-4}, b_{10} = -4.5 \times 10^{-10}, b_{11} = 2.6 \times 10^{-4}, b_{12} = -1.6 \times 10^{-4}, b_{13} = 7.2 \times 10^{-5}$

Fig. 10 shows the step response of 1kW in the forward direction. Due to the specifications of the prototype, the maximum possible variation that can be safely applied to the system is 25%. Figs 11 and 12 show the response of the system under 25% parameter variation in tuning capacitance C_T and tuning inductor L_T and L_{si} respectively. It is evident from these results that there is no significant variations from the nominal system as shown by the simulation results in Section 4.1 and thus validating the performance capabilities of the robust controller.

In order to improve the settling time of the controller, a second experiment was performed using a reduced second order controller, based on the Hankel singular value (SV) based reduction algorithm. Hankel SV's can be used to determine the dominant energy states of a stable system, which are preserved while states of lower energy are removed. Fig. 13 shows the results of the second order reduced order controller in comparison with the H$_\infty$robust controller for the nominal system. It can be seen that reducing the order of the controller results in some improvement in the settling time of the controller.

5. Conclusions

Due to their high order and nonlinear nature, the performance of bidirectional IPT systems degrade significantly with changes in systems parameters when controlled with conventional PID controllers. Therefore, a robust H_∞ controller has been designed to reduce the effects of parametric uncertainties on power regulation as well as to eliminate tedious tuning procedures associated with PID controllers. Several objective functions including settling time, rise time and peak overshoot, were minimized using LMI techniques to obtain the optimal H_∞ controller whist maintaining robust stability and tracking. Simulations using MATLAB as well as experimental tests were conducted to verify the response of the robust controller.

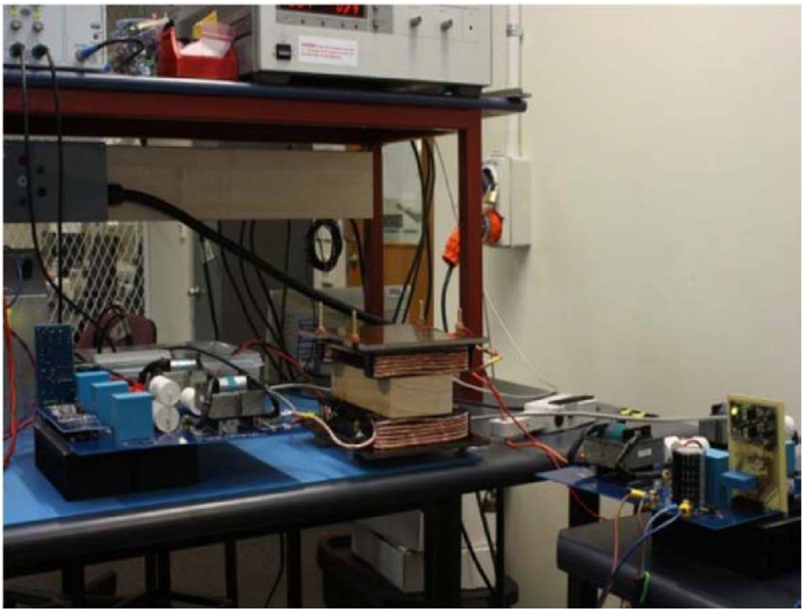

Figure 9: Prototype Bidirectional IPT system used for verification

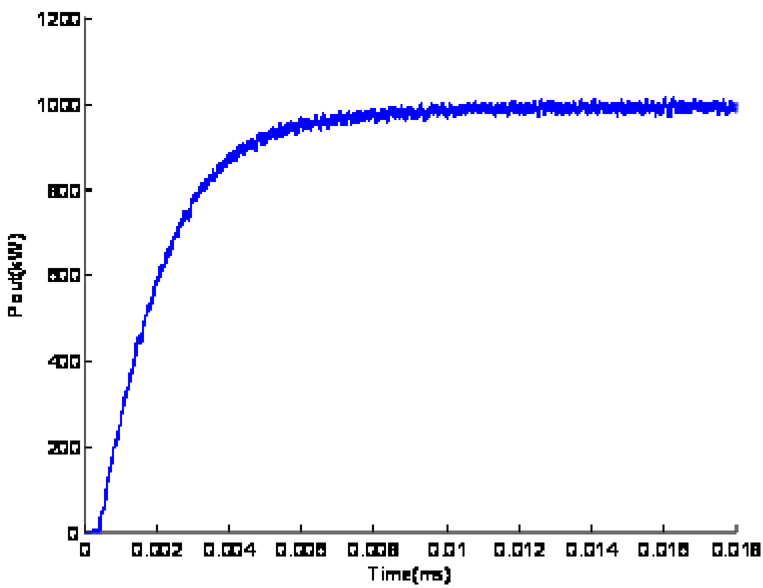

Figure 10: Experimental results of robust controller for nominal system

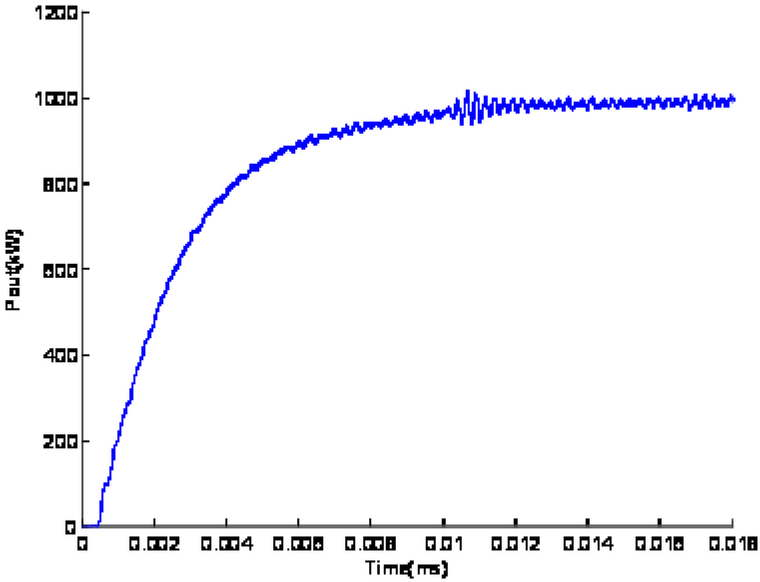

Figure 11: Experimental result of robust controller for system with 25% C_T variation

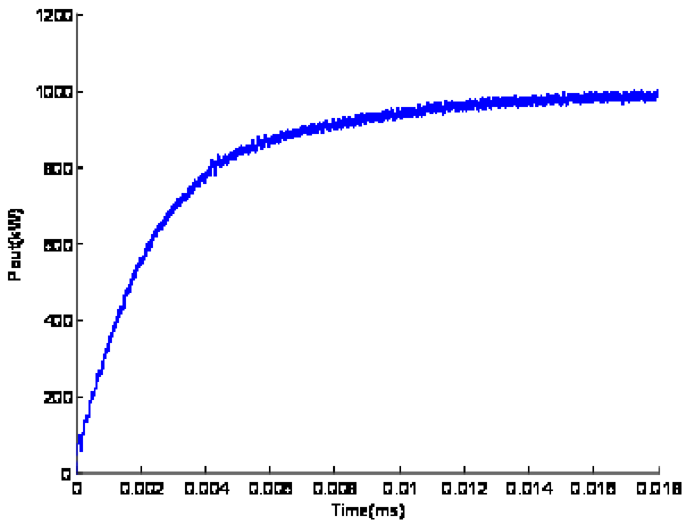

Figure 12: Experimental result of robust controller for system with 25% L_T and L_{si} variation

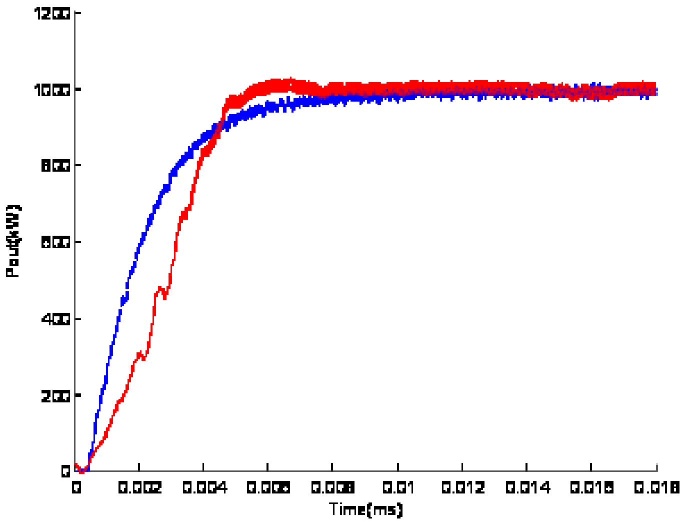

Figure 13: Experimental result of robust controller (blue) and reduced order (2nd order) robust controller (red) for nominal system

References

[1] G.J. BALAS, A.K. PACKARD, M.G. SAFONOV and R.Y. CHIANG: Next generation of tools for robust control. In *Proc. of the American Control Conf.*, **6** (2004), 5612-5615.

[2] J. DOYLE and G. STEIN: Multivariable feedback design: Concepts for a classical/modern synthesis. *IEEE Trans. on Automatic Control*, **26**(1), (1981), 4-16.

[3] A. W. GREEN and J. T. BOYS: 10 kHz inductively coupled power transfer-concept and control. In *Fifth Int. Conf. on Power Electronics and Variable-Speed Drives*, (1994), 694-699.

[4] DA-WEI GU, P. PETKOV and M. KONSTANTINOV: Robust Control Design with MATLAB. Springer-Verlag London, ISBN-10: 1852339837, 2005.

[5] HAO HAO, G.A. COVIC and J.T. BOYS: A parallel topology for inductive power transfer power supplies. *IEEE Transactions on Power Electronics*, **29**(3), (2014), 1140-1151.

[6] JR-UEI WILLIAM HSU, AIGUO PATRICK HU, P. SI and AKSHYA K. SWAIN: Power flow control of a 3-D wireless pick-up . In *2nd IEEE Conf. on Industrial Electronics and Applications*, (2007), 2172-2177.

[7] JR-UEI WILLIAM HSU, AIGUO PATRICK HU and AKSHYA SWAIN: A wireless power pickup based on directional tuning control of magnetic amplifier. *IEEE Trans. on Industrial Electronics*, **56**(7), (2009), 2771-2780.

[8] JR-UEI WILLIAM HSU, AIGUO PATRICK HU and AKSHYA SWAIN: Fuzzy logic based directional full-range tuning control of wireless power pickups . *IET Power Electronics*, **5**(6), (2012), 773-781.

[9] JR-UEI WILLIAM HSU, AIGUO PATRICK HU and AKSHYA K. SWAIN: Fuzzy based directional tuning controller for a wireless power pick-up . In *EEE Region 10 Conference*, (2008).

[10] JR-UEI WILLIAM HSU, AKSHYA K SWAIN and AIGUO PATRICK HU: Implicit adaptive controller for wireless power pick-ups . In *6th IEEE Conf. on Industrial Electronics and Applications*, (2011), 514-519.

[11] C.-Y. HUANG, J.T. BOYS and G.A. COVIC: LCL pickup circulating current controller for inductive power transfer systems. *IEEE Trans. on Power Electronics*, **28**(4), (2013), 2081-2093.

[12] LIANG HUANG, A. PATRICK HU and AKSHYA SWAIN: A New Resonant Compensation Method for Improving the Performance of Capacitively Coupled Power Transfer System . In *IEEE Energy Conversion Congress and Exposition*, (2014), 870-875.

[13] LIANG HUANG, A. PATRICK HU and AKSHYA SWAIN: Comparison of Two High Frequency Converters for Capacitive Power Transfer . In *IEEE Energy Conversion Congress and Exposition*, (2014), 5437-5443.

[14] LIANG HUANG, AIGUO PATRICK HU and AKSHYA SWAIN: An overview of capacitively coupled power transfer-a new contactless power transfer solution . In *8th IEEE Conf. on Industrial Electronics and Applications*, (2013), 461-465.

[15] J.V. INGLES, P. GARCES and R. LEYVA: Robust LMI control of a buck-boost converter with low ripple propagation. In *20th Mediterranean Conf. on Control Automation*, (2012), 1272-1277.

[16] S.M. ASIF IQBAL, U.K. MADAWALA, D.J.THRIMAWITHANA and AKSHYA K. SWAIN: A Bi-directional inductive power transfer system with individually controlled tracks and pick-ups . In *IEEE Energy Conversion Congress and Exposition Asia*, (2013), 1059-1064.

[17] N.A. KEELING, J.T. BOYS and G.A. COVIC: Unity power factor inductive power transfer pick-up for high power applications. In *34th Annual Conf. of IEEE Industrial Electronics*, (2008), 1039-1044.

[18] GE LI, YINGUI ZHOU, HAITIAN WANG, PENG FU and LIANG CAO: Compact power supplies for tokamak heating. *IEEE Transactions on Dielectrics and Electrical Insulation*, **19**(1), (2012), 233-238.

[19] YAN-LING LI, YUE SUN and XIN DAI: μ-synthesis for frequency uncertainty of the ICPT system. *IEEE Transactions on Industrial Electronics*, **60**(1), (2013), 291-300.

[20] YANN-LING LI, YUE SUN and XIN DAI: Robust control for an uncertain LCL resonant ICPT system using LMI method. *Control Engineering Practice*, **21**(1), (2013), 31-41.

[21] RENQUAN LU, SHUKUI LI and LIN XUE: Robust H_∞; optimal speed control of DC motor using lmi approach. In *Control and Decision Conf.*, (2008), 4350-4354.

[22] B. MORGAN JR.: Sensitivity analysis and synthesis of multivariable systems. *IEEE Trans. on Automatic Control*, **11**(3), (1966), 506-512.

[23] M.J. NEATH, A.K. SWAIN, U.K. MADAWALA and D.J. THRIMAWITHANA: An optimal PID controller for a bidirectional inductive power transfer system using multiobjective genetic algorithm. *IEEE Transactions on Power Electronics*, **29**(3), (2014), 1523-1531.

[24] M.J. NEATH, A.K. SWAIN, U.K. MADAWALA, D.J. THRIMAWITHANA and D.M. VILATHGAMUWA: Controller synthesis of a bidirectional inductive power interface for electric vehicles. In *IEEE Third Int. Conf. on Sustainable Energy Technologies*, (2012), 60-65.

[25] C. OLALLA, R. LEYVA, A. EL-AROUDI and I. QUEINNEC: Robust LQR control for PWM converters: An LMI approach. *IEEE Trans. on Industrial Electronics*, **56**(7), (2009), 2548-2558.

[26] G. SCHEIBLE, D. DZUNG, J. ENDRESEN and JAN-ERIK FREY: Unplugged but connected [design and implementation of a truly wireless real-time sensor/actuator interface]. *IEEE Industrial Electronics Magazine*, **1**(2), (2007), 25-34.

[27] PING SI, A.P. HU, S. MALPAS and D. BUDGETT: A frequency control method for regulating wireless power to implantable devices. *IEEE Trans. on Biomedical Circuits and Systems*, **2**(1), (2008), 22-29.

[28] S. SKOGESTAD and I. POSTLETHWAITE: Multivariable Feed Back Control: Analysis and Design. Wiley, second edition, 2005.

[29] J.P.C. SMEETS, T.T. OVERBOOM, J.W. JANSEN and E.A. LOMONOVA: Comparison of position-independent contactless energy transfer systems. *IEEE Trans. on Power Electronics*, **28**(4), (2013), 2059-2067.

[30] A.K. SWAIN, M.J. NEATH, U.K. MADAWALA and D.J. THRIMAWITHANA: A dynamic multivariable state-space model for bidirectional inductive power transfer systems. *IEEE Trans. on Power Electronics*, **27**(11), (2012), 4772-4780.

[31] AKSHYA SWAIN, DHAFER ALMAKHLES, YOUFENG HOU, NITISH PATEL and UDAYA MADAWALA: A sigma-delta modulator based PI controller for bi-directional inductive power transfer system, . In *2nd IEEE Southern Power Electronics Conf.*, (2017), 1-5.

[32] AKSHYA SWAIN, DHAFER ALMAKHLES, NATHAN PYLE, HOSSEIN MEHRABI and AIGUO PATRICK HU: Single-bit modulator based controller for capacitive power transfer system. In *2nd IEEE Southern Power Electronics Conf.*, (2017), 1-5.

[33] AKSHYA SWAIN, SRIKANTH DEVARAKONDA and UDAYA MADAWALA: Modelling, sensitivity analysis and controller synthesis of multi pick-up bi-directional inductive power transfer systems. *IEEE Trans. on Industrial Informatics*, **10**(2), (2014), 1372-1380.

[34] AKSHYA K. SWAIN, MICHAEL J. NEATH, U.K. MADAWALA and D.J.THRIMAWITHANA: A dynamic model for bi-directional inductive power transfer systems. In *37th IEEE Conf. on Industrial Electronics Society*, (2011), 1024-1029.

[35] G. WILLMANN, D.F. COUTINHO, L. F A PEREIRA and F.B. LIBANO: Multiple-loop H_∞ control design for uninterruptible power supplies. *IEEE Trans. on Industrial Electronics*, **54**(3), (2007), 1591-1602.

[36] H.H. WU, A. GILCHRIST, K. SEALY, P. ISRAELSEN and J. MUHS: A review on inductive charging for electric vehicles. In *Int. Electric Machines Drives Conf.*, (2011), 143-147.

[37] M. YILMAZ and P.T. KREIN: Review of the impact of vehicle-to-grid technologies on distribution systems and utility interfaces. *IEEE Trans. on Power Electronics*, **28**(12), (2013), 5673-5689.

[38] LIU YU-ZHONG, LIN LU and LI YAN: H_∞ dynamical output feedback control of switched systems with delayed perturbations. In *Control and Decision Conf.*, (2009), 881-884.

[39] LAN ZHOU, JIN HUA SHE, MIN WU and YONG HE: LMI-based design method of robust modified repetitive-control systems. In *8th IEEE Int. Conf. on Control and Automation*, (2010), 440-445.